Proceedings of ASME 2021 40th International Conference on Ocean, Offshore and Arctic Engineering OMAE 2021 June 21-30, 2021, Virtual, online

OMAE2021-63701

ADVANCES ON REDUCED-ORDER MODELING OF FLOATING OFFSHORE WIND TURBINES

Frank Lemmer, Wei Yu, Heiner Steinacker

Stuttgart Wind Energy (SWE)
University of Stuttgart
70569 Stuttgart, Germany
lemmer@ifb.uni-stuttgart.de

Danai Skandali, Steffen Raach

sowento GmbH
70569 Stuttgart, Germany
raach@sowento.com

ABSTRACT

Aero-hydro-servo-elastic modeling of Floating Offshore Wind Turbines (FOWTs) is a key component in the design process of various components of the system. Different approaches to order reduction have been investigated with the aim of improving structural design, manufacturing, transport and installation, but also the dynamic behavior, which is largely affected by the blade pitch controller. The present work builds on previous works on the SLOW (Simplified Low-Order Wind Turbine) code, which has already been used for the above purposes, including controller design. While the previous rigid rotor model gives good controllers in most cases, we investigate in the present work the question if aero-elastic effects in the design model can improve advanced controllers. The SLOW model is extended for the flapwise bending and coupled to NREL's AeroDyn, linearized and verified with the OlavOlsen OO-Star Wind Floater Semi 10MW public FOWT model. The results show that the nonlinear and linear reduced-order SLOW models agree well against OpenFAST. The state-feedback Linear Quadratic Regulator (LQR) applied with the same weight functions to both models, the old actuator disk, and the new aero-elastic model shows that the LQR becomes more sensitive to nonlinear excitation and that the state feedback matrix is significantly different, which has an effect on the performance and potentially also on the robustness. Thus modeling uncertainties might even be more critical for the LQR of the higher-fidelity model.

INTRODUCTION

Floating Offshore Wind Turbines (FOWTs) are on the verge of becoming a key technology for offshore wind energy generation. After the successful demonstration of single turbines and wind farms, the technology stage is now about advancing on the learning curve in terms of supply chain, manufacturing, installation but also in terms of design. Current works, including the CarbonTrust Joint Industry Project [1], investigate numerical modeling of FOWTs and its interfaces within the design of floater, moorings and secondary components. A repeatedly mentioned limitation of the current practice is a highly iterative process, computationally demanding coupled simulations and a lack of integration of all components into a streamlined design and simulation process.

Various researchers have addressed the topic of order-reduction for FOWT numerical models [2, 3, 4, 5, 6, 7]. Coupled aero-hydro-servo-elastic simulation models with an adapted modeling depth or fidelity shall be designed in order to benefit from the maximum computational efficiency for each design task. For controller design, many authors address a simplified linearized state-space formulation, which has the actuated variables (blade pitch, generator torque) as input. For structural design tasks, tools with few parameters and a standardized setup process allow the design engineer to run numerous sensitivity studies and optimizations during the conceptual stage. The present model is being developed with the goals of achieving an 1) optimal understanding of the FOWT dynamics through linearized state-space models, 2) standardized repeatable design process and 3) Multidisciplinary Design Optimization (MDO). The understanding of the linear dynamics is very important for advanced state feedback blade pitch and generator torque controllers, which will be the use case for the model demonstration in the present paper.

Modeling

The methodology of the present work and the SLOW model in general is a "white box", first-principles-based, modeling of the aero-hydro-servo-elastic phenomena. We build on the existing SLOW environment by University of Stuttgart and sowento [4, 8, 9], extending it for additional aero-elastic effects. The main objective of the model is to represent not more than the driving effects for the overall system dynamics and key loads at a high computational efficiency. The symbolic computation of the Equations of Motion (EQM) is a decisive element leading to its high speed of time-domain integration (1hr simulation completes in 3 s). Symbolic programming computes the right hand-side of the EQM in terms of symbolic variable names and therefore no further algebraic calculations and iterations are necessary in each timestep. A symbolic linearization is performed, calculating the Jacobians of the components of the right hand-side expressions. Additional coefficients, representing the linearized partial derivatives of external forces, with respect to states and inputs is necessary in the case of linearization (see Figure 2).

SLOW uses the theory of Flexible Multibody Systems (FMBS) for the structural dynamics modeling including large reference motion. Hydrodynamics use linear potential flow coefficients with a simplified representation of radiation effects. The constant matrix approach by Taghipour [10] significantly accelerates time-domain and frequency-domain computations and is valid for most FOWT platforms [4]. Viscous effects can be modeled with Morison's equation. In this work, only linear generalized damping coefficients are used, as given with the concept specifications, in order to simplify and focus on aero-elastic effects. The hydrodynamics module of SLOW uses NREL's MoorDyn [11] to compute a lookup table of forces, as function of horizontal and vertical fairlead displacements from the anchor. The quasi-static model is linearized for the linear formulation. The conventional aerodynamic model of SLOW uses a look-up table of rotor power and thrust coefficients. These are stored as function of the Tip-Speed Ratio (TSR) and the blade pitch angle and give the rotor thrust and torque, acting on the FMBS. The generator torque controller and the blade pitch controller is included in both, nonlinear and linearized models.

Although the floater has often been modeled as rigid body in coupled tools, more and more studies reveal the need for an improved modeling of the floater, representing structural elasticities and an estimate of fatigue loads within the structure [12, 13, 14]. The methodology of the present study on elastic blades can be applied in the same way for the elastic floater, modeled by beams. The only limitation for the present model is to find few, meaningful DOFs in order to keep the computational efficiency, which only holds for low-order systems, due to the symbolic programming.

OpenFAST has recently been extended to take into account the floating platform dynamics in the linearization [15]. It is thus possible to use OpenFAST to obtain linearized state-space models for all DOFs and subsets thereof. The input of wave forces is also possible, based on a parametric wave force transfer function, as in SLOW [16, 17]. The radiation model has to be modeled as an identified state-space model from the potential flow model. The reason to work with and extend SLOW nonetheless are 1) the ability to flexibly define the Multibody System layout, even for unconventional systems (multi-turbine floaters, multi-rotor turbine), 2) the ability to add DOFs as necessary, 3) the ability to investigate new approaches, like harmonic and stochastic linearization [2] and 4) the computational performance of the nonlinear time-domain model for quick load analyses and sensitivity studies.

Controls

Controls are the target application of the extended reduced-order modeling of the present paper. The task of controller design for FOWTs is especially critical and reported repeatingly because of a potential "negative damping" of the FOWT in the platform pitch mode. The negative damping is due to a transfer zero from blade pitch angle to rotor speed in the right half-plane [18, 19]. Several controller design approaches have been considered. Standard Proportional-Integral (PI) controllers on the one hand, need to be detuned for a reduced bandwidth, in order not to excite the right half-plane zeros [20, 21, 8, 22, 23]. The reduced controller bandwidth has the side effect that the tracking of the rotor speed is often unsatisfactory. It leads to large power and drivetrain load fluctuations.

For an improved controller performance, multivariable controllers can be applied, which feed back not only one signal but, next to the rotor speed, tower-top or platform motion signals for improved damping [24, 25, 26, 27, 28, 29, 23]. These controllers are often state feedback controllers, which require measurements of all states of the controller design model. If these states cannot be measured directly, an observer is necessary, which reconstructs the missing measurements through a dynamic model [30]. The drawback of state feedback controllers, like the Linear Quadratic Regulator (LQR) used in this work, is that they are particularly dependent on the controller design model and its agreement with the physical model. As a consequence, these controllers are often less robust against unmodeled dynamics or uncertain parameters. This is the reason, why advanced controllers need high-quality dynamic models, which are still not too detailed and too computationally demanding to be applicable for the controller design task.

We have seen in earlier works that the LQR for FOWTs can have problems when the tower natural frequency is very close to the three-times-per-revolution (3p) frequency. This is often the case for FOWTs with catenary moorings because the tower has, when placed on a floating platform, an increased natural frequency, compared to a cantilevered tower. Thus, the soft-stiff design with a tower natural frequency in-between the 1p and 3p frequencies is often not possible or not economical anymore. In addition, the blade natural frequencies are often close to the 3p and tower frequencies. For this reason, we decided to investigate an increase in model fidelity adding one flapwise Degree of Freedom (DOF) for each blade for the linearized controller design model.

MODELING APPROACH

The model uses the Newton-Euler formalism, which is a way to construct equations of motion of MBS in an automated way, based on user-defined bodies (rigid and flexible) and DOFs [31]. In the present work, the floater and tower DOFs shown in Figure 1, are the same as in the thorough verification [4] and validation [8]. In this work, one flapwise DOF for each blade is added. Thus, the previous rigid body of the rotor is replaced by a rigid body for the hub and three elastic beams for the rotor blades. The Newton-Euler formalism assumes six generalized coordinates for each rigid and flexible body. Rigid bodies are defined in the inertial frame, whereas elastic bodies are defined in the reference frame (due to numerical reasons). Elastic bodies have, in addition to the six rigid generalized coordinates, an elastic generalized coordinate for each of the defined DOFs. Here, only one DOF per blade, in flapwise direction, is applied, where the mode shape is used as a shape function. In the final step of the setup of the equations of motion, the Newton-Euler equations in the generalized coordinates of each body are transformed into minimal coordinates, meaning the set of DOFs, which is here platform surge, heave and pitch, rotor rotation, the generalized tower fore-aft deformation, the blade flapwise generalized deformation and the blade pitch actuator angle.

$$\mathbf{q} = [x_p,\, z_p,\, \beta_p,\, \varphi,\, x_t,\, x_b,\, \theta_1]^T\,. \qquad (1)$$

The properties of the blades, necessary for the MBS dynamic equations are pre-calculated, according to the Standard Input Data (SID) format [32]. Part of the SID are, for example, the entries of the generalized mass matrix for each body, containing rigid-body masses, inertia but in addition also the generalized elastic mass, as well as its translational and rotational couplings. The generalized stiffnesses include geometric stiffening as function of the rotor speed. These properties can be pre-computed because the Newton-Euler equations are written in the reference frame of the elastic body, called also the Floating Frame of Reference.

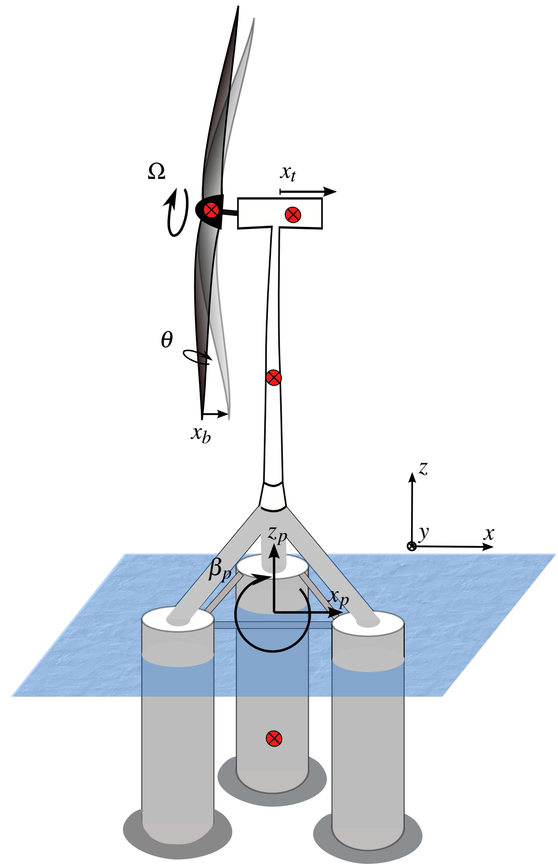

FIGURE 1. MECHANICAL SKETCH OF REDUCED-ORDER MULTIBODY SYSTEM OF THIS WORK.

Nonlinear aero-elastics

The structural dynamics model has been interfaced with AeroDyn v13 [33, 34]. For this purpose, a C-code wrapper function, which initializes all derived types of Aerodyn as described in [34], was built. This wrapper can be called from Matlab, which is convenient for a standalone execution and transfer of all model inputs as arguments. Data types are then transferred to Fortran using the `ISO_C_Binding` library.

The inputs to the structural model (and outputs from AeroDyn wrapper) are the six generalized rigid-body forces in the (pitched and coned) blade root system. The outputs of the structural model (and inputs to AeroDyn wrapper) are the blade root reference frame kinematics (position, velocity, angular velocity and rotation tensor), as well as shape functions and associated DOFs. This is a slightly different interface, compared to the new OpenFAST modularization framework [35, p. 5], see Table 1.

The description of rotations in the calculation of blade root

TABLE 1. INPUTS AND OUTPUTS TO AND FROM AERODYNAMIC MODULE.

	SLOW	OpenFAST [35]
In	Blade root kinematics shape function, gen. coordinates	Nodal kinematics along blade
Out	Generalized forces (3 transl., 3 rot. of ref. frame, generalized elastic forces)	Distributed forces along blade per unit-length

and nodal kinematics of the blades turned out to be of importance. In the present model, Kardan angles are used, which is different to the rotations in ElastoDyn of OpenFAST, where triconometric functions are avoided in the rotation tensors, see [36, p. 15].

Linearized aero-elastics

The linearization of the dynamic equations of the entire aero-hydro-servo-elastic FOWT model is done about the set-points of states $\mathbf{x}_0$, disturbance and control inputs $\mathbf{u}_0$ as

$$\mathbf{x} = \mathbf{x}_0 + \Delta\mathbf{x} \qquad \mathbf{u} = \mathbf{u}_0 + \Delta\mathbf{u}, \tag{2}$$

where $\Delta\mathbf{x}$ and $\Delta\mathbf{u}$ are the new vectors of differential states and inputs, respectively. For the following linear model descriptions, the Δ-symbol will be omitted. The coupled linearized state-space model can then be written with the generalized mass Matrix $\mathbf{M}$ and the position- and velocity-dependent forces $\mathbf{Q}$ and $\mathbf{P}$, respectively as

$$\dot{\mathbf{x}} = \underbrace{\begin{bmatrix} \mathbf{0} & \mathbf{E} \\ -\mathbf{M}^{-1}\mathbf{Q} & -\mathbf{M}^{-1}\mathbf{P} \end{bmatrix}}_{\mathbf{A}} \mathbf{x} + \mathbf{B}\mathbf{u}, \tag{3}$$

with the input matrix $\mathbf{B} = [M_g, \theta, v_0, \zeta]^T$. The control inputs are the generator torque M_g, the collective blade pitch angle θ, as well as disturbances rotor-effective wind speed v_0 and wave height ζ. The wave height requires a parametric wave excitation model according to [16]. Linear aerodynamic coefficients are computed through a central difference scheme using the above-mentioned standalone coupling of Matlab and AeroDyn. With the interface of Table 1, the linear generalized aerodynamic forces $\bar{\mathbf{F}}_{b,i}$ are calculated as a Taylor series up to the first order for each blade with the partial derivatives with respect to the blade pitch angle θ, the rotor-effective wind speed v_0 and the generalized elastic blade flapwise velocity $\dot{x}_b$ as

$$\bar{\mathbf{F}}_{b,i} = \frac{\partial \bar{\mathbf{F}}_{b,i}}{\partial \Omega} d\Omega + \frac{\partial \bar{\mathbf{F}}_{b,i}}{\partial \theta} d\theta + \frac{\partial \bar{\mathbf{F}}_{b,i}}{\partial v_0} (dv_0 - \dot{x}_{hub}) + \frac{\partial \bar{\mathbf{F}}_{b,i}}{\partial \dot{x}_b} d\dot{x}_b. \tag{4}$$

The linear model takes into account aerodynamic damping through the consideration of the blade root rigid-body velocity in downwind direction of the inertial frame x_{hub}. All partial derivatives with respect to the azimuth angle φ are neglected in the present formulation and the state-space model is averaged over several set points of φ. This means that all rotor-harmonic effects from gravity or wind shear are neglected with a gain in simplicity, while keeping the structural dynamic coupling of blades and tower.

FIGURE 2. LINEAR AERODYNAMIC HYDRODYNAMIC AND MOORING LINE COEFFICIENTS FOR COUPLED LINEAR STATE-SPACE FOWT MODEL.

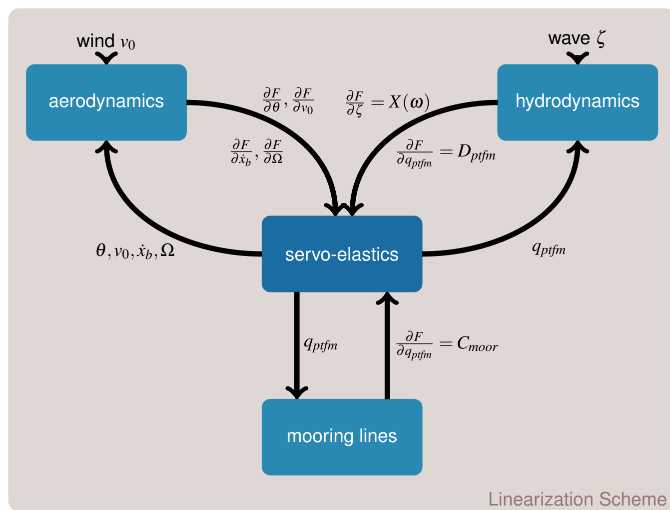

The forces $\bar{\mathbf{F}}_{b,i} \in \mathbb{R}^{7\times1}$ contain the three generalized forces and three moments in the floating frame of reference. Here, the nodal forces from AeroDyn have to be transformed into the reference frame because AeroDyn returns all forces in the twisted nodal frame. The same holds for the computation of the generalized flapwise elastic force, which is weighted with the 3-dimensional shape function of the blade. The latter is the seventh element of $\bar{\mathbf{F}}_{b,i}$. The linear coefficients of Eqn. (4) are computed with a central difference scheme for all operating points. For a first verification, the linear coefficients were compared against the previously used lumped rotor thrust coefficient by summing the coefficients for the three blades ([9, p. 68]). This comparison gives a good agreement for all partial derivatives.

The entire set of linearized coefficients of the submodules aerodynamics, hydrodynamics and mooring is illustrated in Figure 2. The coefficients which are already assumed to be linear in the nonlinear formulation are not shown, like the hydrostatic stiffness. The wave excitation force coefficient $\mathbf{X}(\omega)$ has to be causalized and parameterized, according to [16] for a state-space description. A linear hydrodynamic damping matrix $\mathbf{D}_{ptfm}$ can be obtained from a linearization of Morison drag, see [37]. The quasi-static mooring line model is linearized about each operating point, giving the generalized linearized stiffness matrix with coupling elements with respect to the generalized platform DOFs q_{ptfm}.

Verification

The results of the new model will be exemplarily calculated for the OlavOlsen OOStar Wind Floater Semi 10 MW [38]. The FAST models can be downloaded from [1].

The first comparison addresses the nonlinear FOWT model with a comparison of the response to an Extreme Operating Gust (EOG), according to IEC load case 2.3 [39]. The new aero-elastic model is compared against the conventional rigid rotor model in Figure 3. Besides a small static offset in surge, the agreement is very good, confirming the model setup including kinematics and kinetics. The 3p frequency is visible in the new aero-elastic model, which is an effect of the gravitational force of each blade. This effect is not visible in the rigid rotor model.

The next comparison addresses the nonlinear, the linearized SLOW model and the OpenFAST model in the same EOG in Figure 4. The EOG represents a large nonlinear excitation to the system, which can be challenging, especially for the linear representation of the highly nonlinear aerodynamics. It can be seen that there is a good agreement of the nonlinear SLOW model and the OpenFAST model. The natural frequencies and damping of the platform DOFs, the tower bending and the rotor speed and blade bending are captured very well. Small wiggles of the tower bending at the 3p frequency are not visible in OpenFAST, which will have to be investigated. The surge (x_p) offset of FAST is not a static offset but results from a very lightly damped low-frequency motion. The coupled blade flapwise natural frequency given by the linear SLOW model is 0.31 Hz, which is visible in the FAST results of Figure 6.

APPLICATION AS CONTROLLER DESIGN MODEL

As a final result of the present work, the new aero-elastic model is applied as controller design model for an optimal Linear Quadratic Regulator (LQR). The LQR uses weights on states $\mathbf{Q}$, on control inputs $\mathbf{u}_c$ and on their couplings $\mathbf{N}$. Two LQR are designed with the only difference of the employed linearized FOWT models. Once the conventional rigid rotor model is used and once the new aero-elastic model is used. The employed weights are the same, entering zeros for the entries corresponding to the new states $x_{b,i}$ and $\dot{x}_{b,i}$.

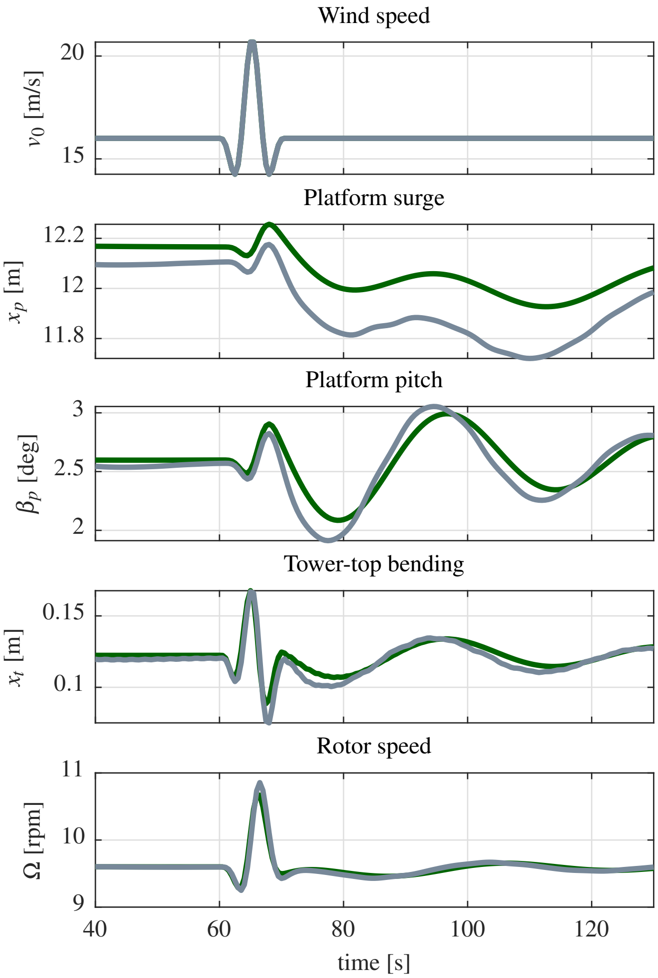

FIGURE 3. NEW AERO-ELASTIC VS. RIGID ROTOR MODEL IN EXTREME OPERATING GUST AT WIND SPEED 16 m/s, RIGID ROTOR (DARK GREEN), ELASTIC BLADES (LIGHT GREY).

Table 2 shows a comparison of the state feedback matrix, which is for the rigid rotor model $\mathbf{K}_{rigid} \in \mathbb{R}^{(2\times12)}$ and the aero-elastic model $\mathbf{K}_{flex} \in \mathbb{R}^{(2\times18)}$. The control law is

$$\mathbf{u}_c = [M_g,\ \theta]^T = \mathbf{K}\mathbf{x}. \quad (5)$$

Only the most relevant gains are shown, without the ones related to surge, heave and the blade pitch actuator. While the first gains on the pitch angle β_p and the integral φ of the rotor speed are

[1] FAST model of OlavOlsen OOStar Wind Floater Semi 10 MW GitHub repository `http://rwt.windenergy.dtu.dk/dtu10mw/dtu-10mw-rwt/-/tree/master/aeroelastic_models`, accessed January 11, 2021.

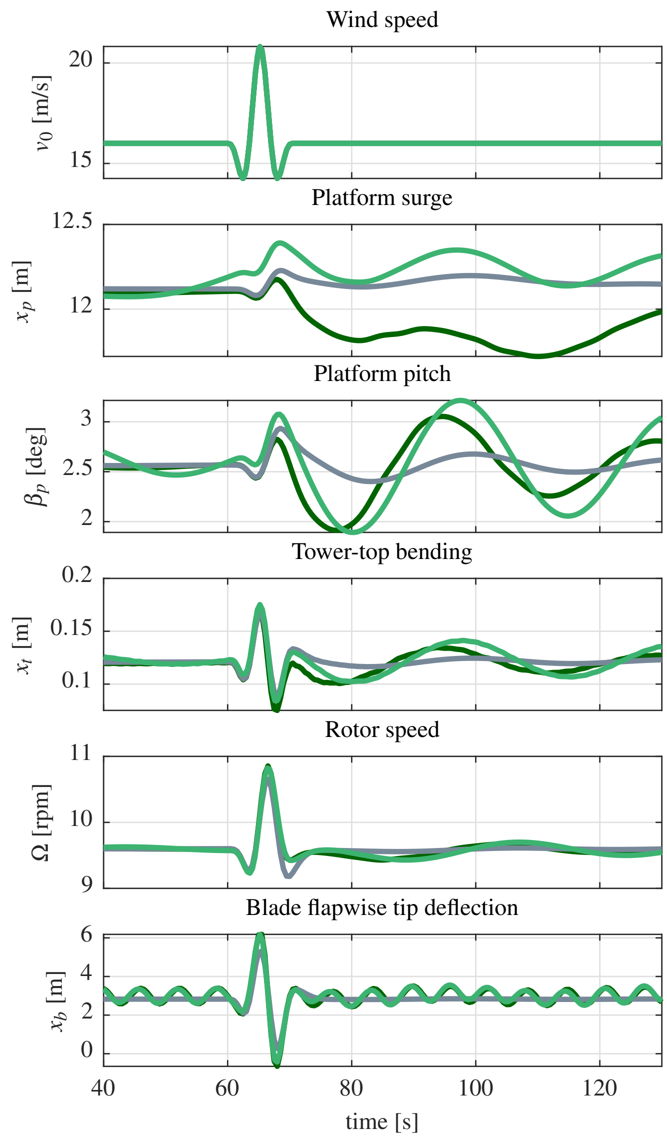

FIGURE 4. NEW NONLINEAR AERO-ELASTIC VS. LINEARIZED MODEL IN EXTREME OPERATING GUST AT WIND SPEED 16 m/s, FAST (LIGHT GREEN), NONLINEAR SLOW (DARK GREEN) AND LINEARIZED MODEL (LIGHT GREY).

equal, the gain of the tower-top bending x_t even changes sign, which might be compensated by the gain of the blade flapwise deformation x_b. The gains on the derivatives, the platform pitch rate of change, the rotor speed and the tower-top velocity are significantly different. This shows the significant influence of the model on the state feedback gains, which has potentially a large influence on the controller performance, as will be shown in the following, but also on its robustness against unmodeled dynamics and uncertain parameters.

An application of the new LQR with FAST in a severe, irregular sea-state [40, Chapter 7] was tested. It turned out that the new LQR is not robust enough for these large excitations, as opposed to the rigid rotor one. The reason of this can be a general reduced robustness of the new controller, designed with the aero-elastic model, against nonlinear effects. On the other hand, a further tuning of the weight matrices could potentially also remedy the problem. This is subject of further investigations.

TABLE 2. COMPARISON OF STATE FEEDBACK MATRIX K FOR RIGID ROTOR AND AERO-ELASTIC MODEL AT 16 m/s.

K_{β_p}	K_{φ}	K_{x_t}	K_{x_b}	$K_{\dot\beta_p}$	K_{Ω}	$K_{\dot x_t}$	$K_{\dot x_b}$
Blade pitch θ, rigid rotor:							
-3.39	-0.27	-0.01		1.04	-2.86	-0.06	
Blade pitch θ, aero-elastic rotor:							
-3.31	-0.27	0.06	-0.003	-3.6	-1.2	0.01	-0.0006

Figure 5 shows the comparison in a turbulent wind simulation at 16 m/s. It can be seen that the LQR designed with the new model gives a satisfactory response. Qualitative observations from the plots are that the new controller reduces the platform pitch and tower-top bending fluctuations, while it leads to increased rotor speed fluctuations. This is confirmed by Figure 6 with the Power Spectral Densities (PSD) of the most relevant signals. The new model leads to lower load amplitudes of the tower, with a comparable magnitude of the flapwise blade deformation. The differences are due to the LQR minimization scheme aiming for the optimal response with both models. The new aerodynamic linearization scheme predicts a larger aerodynamic damping as before (see Fig. 4), which could be the reason for the larger rotor speed fluctuations.

SUMMARY AND CONCLUSIONS

In this work, an existing reduced-order aero-hydro-servo-elastic model for FOWTs has been extended to account for the elastic blade deformation in flapwise direction. The new aero-elastic model has been verified through a comparison against the old model, showing a good agreement. The 3p-effect due to gravitational forces on the blades is visible in the new model but not in the conventional rigid rotor model. The linearized aero-elastic model has been verified through a time-domain comparison in an Extreme Operating Gust (EOG), showing an acceptable performance in spite of the large nonlinear excitation. In a comparison against the higher-fidelity OpenFAST model, the nonlinear model agrees very well, while the linearized model captures the initial response to the gust and fails to predict the decaying behavior afterwards. Nonetheless, the modal analysis of the new linearized model gives accurate coupled natural blade frequencies, compared to OpenFAST.

As a final step, an advanced state-feedback Linear Quadratic Regulator (LQR) was designed for the blade pitch control above

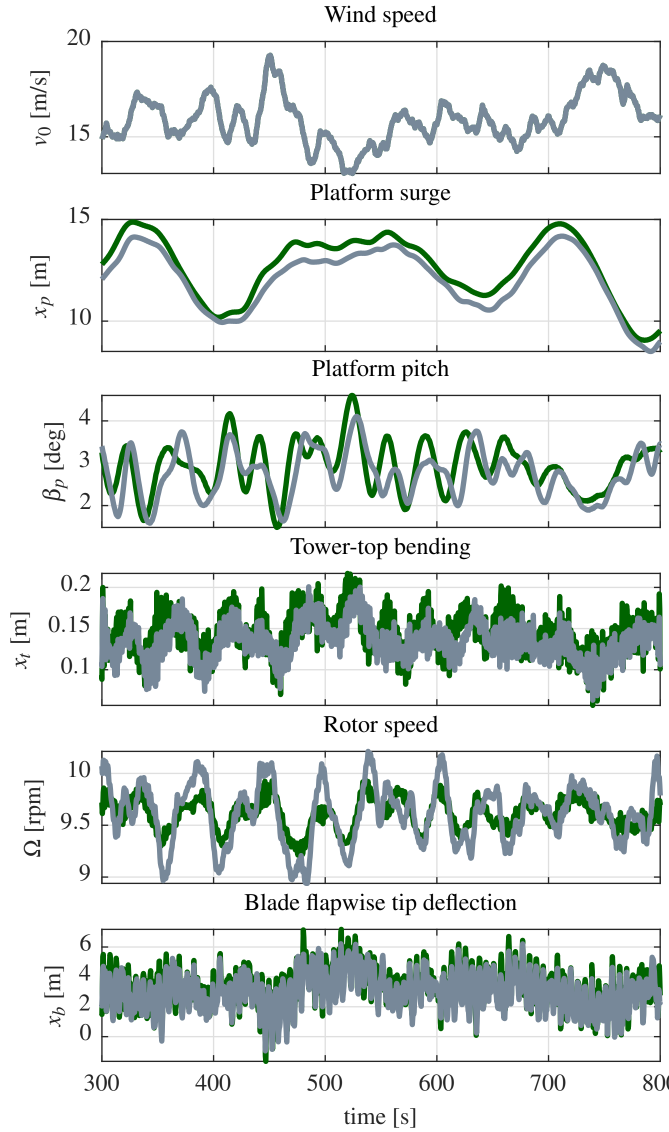

FIGURE 5. FAST TIME-DOMAIN RESULTS WITH ADVANCED STATE-FEEDBACK CONTROLLER (LQR) IN WITH TURBULENT WIND 16 m/s, LQR DESIGNED WITH OLD RIGID BODY MODEL (DARK GREEN) AND DESIGNED WITH NEW AERO-ELASTIC MODEL (LIGHT GREY).

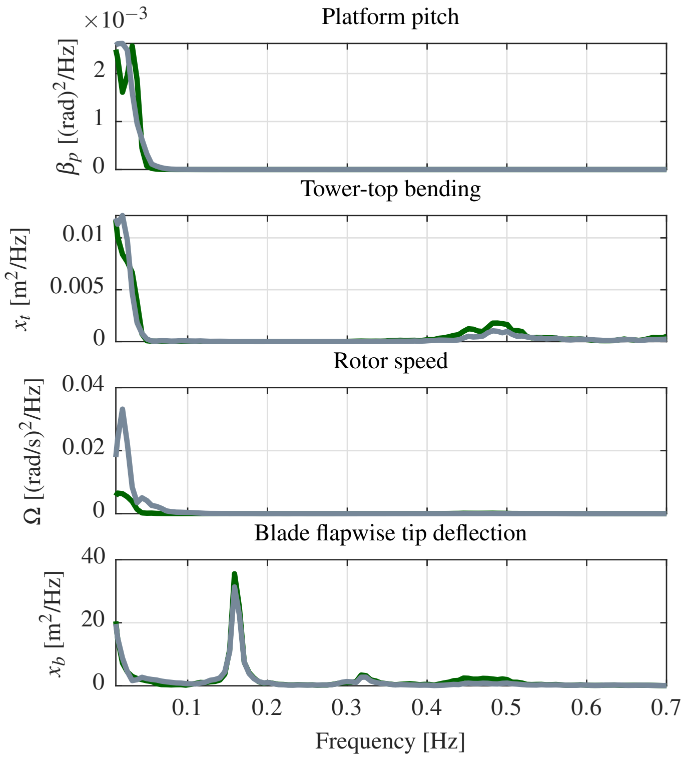

FIGURE 6. FAST POWER SPECTRAL DENSITIES WITH ADVANCED STATE-FEEDBACK CONTROLLER (LQR) IN WITH TURBULENT WIND 16 m/s, LQR DESIGNED WITH OLD RIGID BODY MODEL (DARK GREEN) AND DESIGNED WITH NEW AERO-ELASTIC MODEL (LIGHT GREY).

rated winds. The inital question was if the added physics would improve the controller performance of the LQR, which is designed through an automated algorithm, given a linear state-space model and weight functions. Especially the dynamic coupling of the tower and the blades under 3p excitation appeared to be critical to the authors, prior to the present work. The results of this paper show that the LQR, designed by the new aero-elastic model does put more emphasis on the tower dynamics than the rigid rotor model. However, the rotor speed tracking is clearly reduced. The LQR designed by the new model, however, seems to be less robust against large nonlinear wave excitation. The clear reason for this has to be found in further research.

In conclusion, the extended aero-hydro-servo-elastic modeling proves to be valid, in comparison against OpenFAST. The computational performance is decreased, compared to the rigid rotor model, but is still 7 times more efficient than OpenFAST (with the same DOFs) and can be further increased when applied outside of Matlab (a 10-times speed increase was observed for the rigid body model outside of Matlab). The linear model gives the correct natural frequencies and is therefore a valid model for FOWT controller and observer design, but also for other design tasks like the computation of natural frequencies (Campbell diagram) or real-time load monitoring.

In further steps, the SLOW model will be extended to account for elastic deformation of the floater. This will make it possible to estimate the coupled tower natural frequency more accurately and to estimate structural stresses in an efficient low-order model. Apart from that, the Newton-Algorithm of SLOW will be applied to calculate the equations of motion in the OpenFAST modularization framework. This will allow users, to modify the Multibody System layout (bodies and DOFs), which will be relevant for the emerging advanced multi-turbine and other unconventional designs.

Acknowledgements

The research leading to the presented results was funded partially by the German Federal Ministry for Economic Affairs and Energy (BMWi) within the VAMOS/FLOATEOLE project (FKZ 03EE2004A).

REFERENCES

[1] James, R., 2018. Carbon Trust Floating Wind Joint Industry Project (JIP). Tech. rep., Carbon Trust.

[2] Lupton, R. C., and Langley, R. S., 2020. "Harmonic linearisation of aerodynamic loads in a frequency-domain model of a floating wind turbine". *Wind Energy*.

[3] Fontanella, A., Al, M., Hoek, D. V. D., Liu, Y., and van Wingerden, J.-W., 2020. "A control-oriented wave-excited linear model for offshore floating wind turbines". *Journal of Physics: Conference Series,* ***1618***.

[4] Lemmer, F., Yu, W., Luhmann, B., Schlipf, D., and Cheng, P. W., 2020. "Multibody modeling for concept-level floating offshore wind turbine design". *Multibody System Dynamics,* ***49***(2), pp. 203–236.

[5] Pegalajar-Jurado, A., Borg, M., and Bredmose, H., 2018. "An efficient frequency-domain model for quick load analysis of floating offshore wind turbines". *Wind Energy Science,* ***3***, pp. 693–712.

[6] Wang, K., Ji, C., Xue, H., and Tang, W., 2017. "Frequency domain approach for the coupled analysis of floating wind turbine system". *Ships and Offshore Structures,* ***12***(6), pp. 767–774.

[7] Betti, G., Farina, M., Guagliardi, G., Marzorati, A., and Scattolini, R., 2014. "Development and validation of a control-oriented model of floating wind turbines". *IEEE Transactions on Control Systems Technology,* ***22***(1), pp. 69 – 82.

[8] Lemmer, F., Yu, W., Cheng, P. W., Pegalajar-Jurado, A., Borg, M., Mikkelsen, R., and Bredmose, H., 2018. "The TripleSpar campaign: Validation of a reduced-order simulation model for floating wind turbines". In Proceedings of the ASME 37th International Conference on Ocean, Offshore and Arctic Engineering, ASME.

[9] Lemmer, F., 2018. "Low-Order Modeling, Controller Design and Optimization of Floating Offshore Wind Turbines". PhD thesis, University of Stuttgart.

[10] Taghipour, R., Pérez, T., and Moan, T., 2008. "Hybrid frequency-time domain models for dynamic response analysis of marine structures". *Ocean Engineering,* ***35***(7), pp. 685–705.

[11] Hall, M., 2021. MoorDyn GitHub repository.

[12] Borg, M., Bredmose, H., and Hansen, A. M., 2017. "Elastic deformations of floaters for offshore wind turbines: dynamic modelling and sectional load calculations". In Proceedings of the ASME 36th International Conference on Ocean, Offshore and Arctic Engineering.

[13] Luan, C., Gao, Z., and Moan, T., 2017. "Development and verification of a time-domain approach for determining forces and moments in structural components of floaters with an application to floating wind turbines". *Marine Structures,* ***51***, pp. 87–109.

[14] Jonkman, J., Branlard, E. S., Hall, M., Hayman, G. J., and Robertson, A. N., 2020. Implementation of substructure flexibility and member-level load capabilities for floating offshore wind turbines in OpenFAST. Tech. rep., NREL.

[15] Johnson, N., Jonkman, J., Wright, A., Hayman, G., and Robertson, A., 2019. "Verification of floating offshore wind linearization functionality in OpenFAST". In Proceedings of the EERA Deepwind 2019.

[16] Lemmer, F., Raach, S., Schlipf, D., and Cheng, P. W., 2016. "Parametric wave excitation model for floating wind turbines". *Energy Procedia,* ***94***, pp. 290–305.

[17] Jonkman, J., Wright, A. D., Hayman, G. J., and Robertson, A. N., 2018. "Full-system linearization for floating offshore wind turbines in OpenFAST (pre-print)". In Proceedings of the ASME 2018 1st International Offshore Wind Technical Conference, ASME.

[18] Skaare, B., Hanson, T. D., and Nielsen, F. G., 2007. "Importance of control strategies on fatigue life of floating wind turbines". In Proceedings of the ASME 26th International Conference on Offshore Mechanics and Arctic Engineering.

[19] Veen, G. V. D., Couchman, Y., and Bowyer, R., 2012. "Control of floating wind turbines". In Proceedings of the American Control Conference, pp. 3148–3153.

[20] Larsen, T. J., and Hanson, T. D., 2007. "A method to avoid negative damped low frequent tower vibrations for a floating, pitch controlled wind turbine". *Journal of Physics: Conference Series,* ***75***.

[21] Jonkman, J., 2008. "Influence of control on the pitch damping of a floating wind turbine". In Proceedings of the 46th AIAA Aerospace Sciences Meeting and Exhibit, AIAA.

[22] Abbas, N. J., Wright, A., and Pao, L., 2019. "An update to the national renewable energy laboratory baseline wind turbine controller". In Journal of Physics: Conference Series, Vol. 1452.

[23] Yu, W., Lemmer, F., Schlipf, D., and Cheng, P. W., 2020. "Loop shaping based robust control for floating offshore wind turbines Loop shaping based robust control for floating offshore wind turbines". *Journal of Physics: Conference Series,* ***1618***.

[24] Fischer, B., 2013. "Reducing rotor speed variations of float-

ing wind turbines by compensation of non-minimum phase zeros". *IET Renewable Power Generation,* ***7***(4), pp. 413–419.

[25] Savenije, F., and Peeringa, J., 2014. "Control development for floating wind". *Journal of Physics: Conference Series,* ***524***.

[26] Schlipf, D., Simley, E., Lemmer, F., Pao, L., and Cheng, P. W., 2015. "Collective pitch feedforward control of floating wind turbines using Lidar". *Journal of Ocean and Wind Energy,* ***2***(4), pp. 223–230.

[27] Lemmer, F., Schlipf, D., and Cheng, P. W., 2016. "Control design methods for floating wind turbines for optimal disturbance rejection". *Journal of Physics: Conference Series,* ***753***.

[28] Okada, Y., Haneda, K., Chujo, T., and Ohtsuka, T., 2019. "Parameter-varying modeling and nonlinear model predictive control for floating offshore wind turbines". *IFAC-PapersOnLine,* ***52***(16), pp. 382–387.

[29] Al, M., Fontanella, A., van der Hoek, D., Liu, Y., Belloli, M., and van Wingerden, J.-W., 2020. "Feedforward control for wave disturbance rejection on floating offshore wind turbines". *Journal of Physics: Conference Series,* ***1618***, p. 022048.

[30] Abbas, N. J., and Pao, L., 2019. "On the controllability of a floating offshore wind turbine". In Journal of Physics: Conference Series, Vol. 1452.

[31] Schiehlen, W., and Eberhard, P., 2014. *Applied Dynamics*, 1st ed. Springer International Publishing.

[32] Wallrapp, O., 1994. "Standardization of flexible body modeling in multibody system codes, part I: Definition of standard input data". *Mechanics of Structures and Machines,* ***22***(3), pp. 283–304.

[33] Moriarty, P. J., and Hansen, C., 2005. AeroDyn theory manual. Tech. rep., National Renewable Energy Laboratory, Golden, USA.

[34] Jonkman, B., and Jonkman, J., 2013. Addendum to the user's guides for FAST, A2AD, and AeroDyn. Tech. rep., NREL.

[35] Jonkman, J., and Jonkman, B. J., 2016. "FAST modularization framework for wind turbine simulation: Full-system linearization". *Journal of Physics: Conference Series,* ***753***.

[36] Jonkman, J., 2007. "Dynamics modeling and loads analysis of an offshore floating wind turbine". PhD thesis, University of Colorado.

[37] Lemmer, F., Yu, W., and Cheng, P. W., 2018. "Iterative frequency-domain response of floating wind turbines with parametric drag". *Journal of Marine Science and Engineering,* ***6***(4).

[38] Pegalajar-Jurado, A., Madsen, F. J., Borg, M., and Bredmose, H., 2018. LIFES50+ D4.5 State-of-the-art models for the two LIFES50+ 10MW floater concepts. Tech. rep., DTU.

[39] IEC, 2019. 61400 Wind turbines - Part 3-1: Design requirements for offshore wind turbines.

[40] Krieger, A., Ramachandran, G. K. V., Vita, L., Gómez Alonso, P., Berque, J., and Aguirre-Suso, G., 2016. LIFES50+ D7.2 Design basis. Tech. rep., DNV-GL.